INTERNATIONAL JOURNAL FOR NUMERICAL METHODS IN FLUIDS, VOL. 4, 321–336 (1984)

A PRACTICAL METHOD OF TWO-EQUATION TURBULENCE MODELLING USING FINITE ELEMENTS

R. M. SMITH

Central Electricity Generating Board, Berkeley Nuclear Laboratories, Berkeley, Gloucestershire GL13 9PB, England

SUMMARY

Incorporation of the k–ε turbulence model into Galerkin finite-element fluid-flow codes (which, unlike upwind finite-difference codes, have no artificial damping) can lead to severe iterative convergence difficulties. This paper introduces an alternative turbulence model (the q–f model) and an associated finite-element discretization method which are designed to overcome these problems. The new model forms the basis of a finite-element fluid-flow code which is robust and efficient. Furthermore, it is demonstrated on a practical example that the code can give good agreement with experiment on fairly coarse meshes.

1. INTRODUCTION

The finite-element (FE) method has been very successful in the analysis of incompressible laminar flows.[1,2] Extension to turbulent flow in complex geometry requires the use of a model which can account for transport of turbulence quantities, for the turbulent stresses are not in general locally determined. The most widely used such model is the k–ε model.[3] This relates the turbulent stresses to the mean rates of strain by use of an eddy viscosity, which is determined by the solution of transport equations in k (the turbulence energy) and ε (the turbulence energy dissipation rate). These equations have generally been solved using upwind finite-difference codes[4] which invariably contain some damping due to numerical diffusion. Incorporation of the k–ε model into Galerkin-FE codes (which have no artificial damping) can lead to a number of difficulties, and serious problems with iterative convergence have been reported by several authors.[5–7] However, the present author[7] also reported an analysis of the difficulties encountered, and isolated the underlying causes. An important conclusion was that the mathematical form of the k–ε transport equations leads to discretized systems which are highly unstable with respect to fast converging iterative solution methods (e.g. Newton–Raphson iteration). However, mathematical forms for turbulence model equations were suggested that should give numerically stable discretized forms, and the present work develops these ideas further.

The purpose of this paper is to report

(i) the formulation and FE-discretization of a two-equation turbulence model which has been designed to be numerically stable,
(ii) the incorporation of the above model in a practical FE fluid-flow code, and
(iii) the performance and accuracy of the code in the prediction of experimental results in a turbulent recirculating flow.

0271–2091/84/040321–16$01.60

Received 3 May 1983

In the following, all variables are rendered dimensionless with respect to characteristic length L and velocity V (the Reynolds number then being given by $\mathrm{Re} = LV/\nu$ where ν is the dynamic viscosity) and the summation convention is used throughout.

2. DYNAMICAL EQUATIONS

The equations governing the steady two-dimensional (or axisymmetric) flow of an incompressible turbulent fluid are

$$u_m \frac{\partial u_n}{\partial x_m} + \frac{\partial p}{\partial x_n} - \frac{1}{x_2^\alpha}\frac{\partial}{\partial x_m}\left(x_2^\alpha \pi_u \left(\frac{\partial u_m}{\partial x_n} + \frac{\partial u_n}{\partial x_m}\right)\right) + 2\alpha \pi_u \frac{u_2}{x_2^2}\delta_{n2} = 0 \quad \text{for } \mathbf{x} \text{ in } \Omega \tag{1}$$

$$\frac{1}{x_2^\alpha}\frac{\partial}{\partial x_m}(x_2^\alpha u_m) = 0 \quad \text{for } \mathbf{x} \text{ in } \Omega \tag{2}$$

where p is the mean pressure, $\mathbf{u}$ is the mean velocity, and δ_{nm} is the Kronecker delta. In plane geometry ($\alpha = 0$), the velocity components u_1, u_2 are in Cartesian co-ordinate directions x_1, x_2, respectively. In axisymmetric geometry ($\alpha = 1$) the components u_1, u_2 are in the axial direction x_1 and the radial direction x_2, respectively. The dimensionless diffusivity of momentum is given by:

$$\pi_u = (1 + \mu_t)/\mathrm{Re} \tag{3}$$

where μ_t is the dimensionless eddy viscosity. The equations are solved in region Ω subject to boundary conditions of the general form

$$\begin{aligned} \mathbf{u} &= \hat{\mathbf{u}} && \text{for } \mathbf{x} \text{ on } \partial\Omega_1 \quad \text{(walls, inlet)} \\ T_1 &= u_2 = 0 && \text{for } \mathbf{x} \text{ on } \partial\Omega_2 \quad \text{(symmetry line)} \\ T_1 &= T_2 = 0 && \text{for } \mathbf{x} \text{ on } \partial\Omega_3 \quad \text{(general outlet)} \end{aligned}$$

where the notation $\hat{\mathbf{u}}$ indicates a prescribed function of $\mathbf{x}$, $\partial\Omega_1$, $\partial\Omega_2$, $\partial\Omega_3$ is a partition of the boundary $\partial\Omega$ and, if $\mathbf{n}$ is the outward pointing normal to $\partial\Omega$, the surface traction $\mathbf{T}$ is defined

$$T_l = \left(-p\,\delta_{lm} + \pi_u\left(\frac{\partial u_l}{\partial x_m} + \frac{\partial u_m}{\partial x_l}\right)\right) n_m \tag{4}$$

3. TURBULENCE MODEL

The above dynamical equations can be solved on specification of the eddy viscosity μ_t, achieved here by the use of a two-equation turbulence model. The variables which have been selected in place of k and ε to characterize the large scale turbulence are q, the (positive) square-root of the turbulence energy and f, a frequency, which can be interpreted as the vorticity of the large scale eddies. Then, the eddy viscosity is given by

$$\mu_t = \mathrm{Re}\, C_\mu q^2/f \tag{5}$$

and the transport equations for q and f are

$$2u_m \frac{\partial q}{\partial x_m} - \frac{1}{x_2^\alpha}\frac{\partial}{\partial x_m}\left(x_2^\alpha \pi_q \frac{\partial K}{\partial x_m}\right) - R_q = Q_q \tag{6}$$

$$u_m \frac{\partial f}{\partial x_m} - \frac{1}{x_2^\alpha}\frac{\partial}{\partial x_m}\left(x_2^\alpha \pi_f \frac{\partial F}{\partial x_m}\right) - R_f = Q_f \tag{7}$$

where

$$K = q^2, \qquad F = f^2 \tag{8}$$

and where the dimensionless diffusivities and sources are defined by

$$\pi_q = l/\sigma_q, \tag{9}$$

$$Q_q = lS_u - C_\mu q^2/l \tag{10}$$

$$\pi_f = C_\mu q^2/(2\sigma_f f^2), \tag{11}$$

$$Q_f = C_\mu C_{1f} S_u - C_{2f} f^2 \tag{12}$$

Here, the quantities σ_q, σ_f, C_μ, C_{1f} and C_{2f} are all constants, the Prandtl–Kolmogorov length scale

$$l = C_\mu |q/f| \tag{13}$$

has been introduced, and the quantity S_u is defined by

$$S_u = \frac{\partial u_n}{\partial x_m}\left(\frac{\partial u_n}{\partial x_m} + \frac{\partial u_m}{\partial x_n}\right) + 2\alpha\left(\frac{u_2}{x_2}\right)^2 \tag{14}$$

The terms R_q and R_f, which represent secondary sources, will be discussed later. An alternative form of equation (7) is

$$u_m \frac{\partial f}{\partial x_m} - \frac{1}{x_2^\alpha}\frac{\partial}{\partial x_m}\left(x_2^\alpha \pi_f' \frac{\partial F'}{\partial x_m}\right) - R_f = Q_f \tag{15}$$

where

$$F' = \ln f^2 \tag{16}$$

and

$$\pi_f' = C_\mu q^2/2\sigma_f \tag{17}$$

These are, of course, analytically equivalent to equations (7), (8) and (11) but they give distinct discretized forms as can be seen in Appendix III. Boundary conditions are of the general form

$$q = \hat{q}, \qquad f = \hat{f} \quad \text{for } \mathbf{x} \text{ on } \partial\Omega_1$$

$$\left(\frac{\partial q^2}{\partial x_m}\right) n_m = 0, \qquad \left(\frac{\partial f^2}{\partial x_m}\right) n_m = 0 \quad \text{for } \mathbf{x} \text{ on } \partial\Omega_2, \partial\Omega_3.$$

The above set of equations are rather different from those commonly used for turbulence modelling. However, with the definition

$$R_q = 2lS_q/\sigma_q, \tag{18}$$

where

$$S_q = \left(\frac{\partial q}{\partial x_m}\right)^2, \tag{19}$$

equation (6) is equivalent to the k transport equation of the familiar k–l one-equation model,[8] σ_q being identified as the turbulent Prandtl number for k. Furthermore, with this choice for R_q and suitable choices for the quantity R_f, the equations set out above (i.e. (5) to (14)) can be made formally equivalent to most two-equation models now in use (e.g. see Appendix I). However, in the present work R_f is taken to be zero, and the resulting turbulence model is termed the q–f model.

The choice of a frequency as the second turbulence parameter in preference to the dissipation rate is not new. Kolmogorov[9] was the first to suggest such a variable, and it has been used in the form $W = f^2$ by Spalding[10] for a k–W model. Saffman[11] also proposed such a model, and this has subsequently been developed into the Wilcox–Traci model.[12] The dissipation rate ε is by far the most widely used second variable, but there does not appear to be any compelling reason for this. It is true that an exact transport equation for the dissipation rate, defined in terms of the fluctuating Cartesian velocity components u_n' by

$$\varepsilon = \frac{1}{\mathrm{Re}} \overline{\left(\frac{\partial u_n'}{\partial x_m}\right)\left(\frac{\partial u_n'}{\partial x_m}\right)}$$

(where the overbar denotes a time average) can be written down, but the closure of the model to eliminate high order correlations results in an equation which could be written down on purely dimensional grounds (e.g. see Reference 13). Also, Launder and Spalding[14] cite an advantage for ε over W or kl, in that no special modelling is required in the fully turbulent region near a wall. However, this is also true of the f variable (with $R_f = 0$). The q–f model would therefore appear equally valid as k–ε with the added advantage, as will be seen later, of numerical stability for the FE-discretized form.

Detailed optimization of most two-equation model constants to obtain the best fit to experimental results has to be carried out by numerical analysis of real flow. However, a good estimate for the value of C_{2f} can be obtained by an analytic solution for the decay of turbulence behind a grid. Similarly, the well known 'log' layer near a solid wall provides a relationship between C_{1f}, C_{2f} and σ_f (see Appendix II). Thus:

$$C_{1f} = C_{2f} - \frac{\kappa^2}{\sigma_f C_\mu^{1/2}} \tag{20}$$

and

$$C_{2f} \sim 1$$

where κ is a constant in the law of the wall (see section 5). If σ_f is of order unity, $C_{1f} \sim 0{\cdot}42$. These values for C_{1f}, C_{2f} agree quite well with those derived from the recommended set of constants for the k–ε model given by Rodi.[3] The values $C_{1f} = C_{1\varepsilon} - 1 = 0{\cdot}44$ and $C_{2f} = C_{2\varepsilon} - 1 = 0{\cdot}92$ are obtained by transforming the source terms of the k–ε equations (Appendix I) into the corresponding terms of the f equation, though since the k–ε and q–f models are not equivalent, the correspondence cannot be exact. There remains some freedom to adjust σ_f around unity, and in fact the values $C_{1f} = 0{\cdot}58$, $C_{2f} = 0{\cdot}92$, $\sigma_q = 1$ and $\sigma_f = 1{\cdot}4$ have been used in the calculation in this paper, as explained in section 7.1.

4. FINITE ELEMENT DISCRETIZATION

The momentum equations (1) are discretized by the Galerkin-FE method in the usual way,[15] with the continuity constraint being handled by a penalty-augmented Lagrangian-multiplier (PALM) method.[16] Eight-noded quadrilateral elements of the serendipity type[17] with quadratic velocity and linear pressure variations are used in the interior of the flow, with special elements at the wall. The former are referred to as 'type 2' whereas the special elements[18] are the types 3 and 4. These have cubic velocity variations perpendicular to the wall and extra nodal variables consisting of the normal gradients of velocity on the grid edge (see Figure 1).

It was shown in Reference 7 that discretizations of non-linear differential equations can

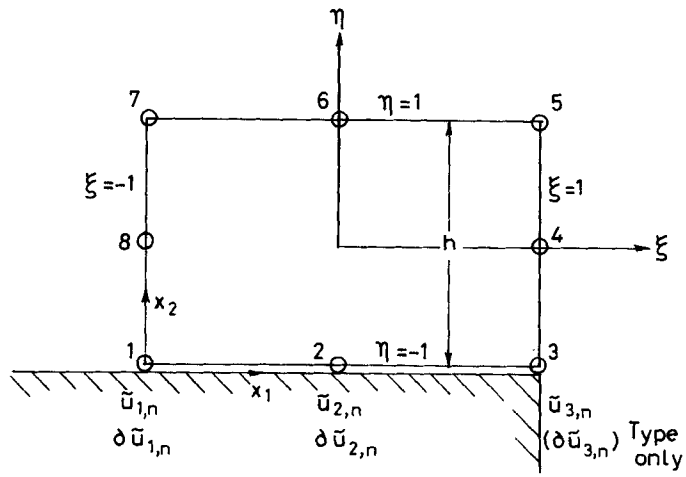

Figure 1. Wall element (type 3 or 4)

have very different properties from the original equations. In particular, multiple discrete solutions can exist in addition to the desired solution, and in a complicated equation system this can lead to very unstable iterative performance. However, it was also suggested, after work by Meyer,[19] that a transport equation (in variable ϕ, say) should produce a stable discrete form provided that

(i) diffusivity is positive everywhere in Ω and for all admissible values of ϕ, and
(ii) the source is monotonic decreasing in ϕ everywhere in Ω.

The q–f transport equations (6) and (7) have been chosen to comply with these requirements. Neglecting convection and the secondary source terms R_f, it is easy to see that Q_f is monotonic decreasing with f^2 and that π_f (the diffusivity of f^2) is positive for all $q \neq 0$ and $f < \infty$. Similarly for the q equation when $l > 0$ is held constant. Provided that the discretization preserves these qualities, stable iterative performance can be expected of each individual equation.

The discretization used for the q–f model equations is as follows. The variables q, f, K and F (equations (8)) are interpolated by the same basis functions as used for the velocity components, whereas the quantities π_u, π_q, π_f, l, Q_q, Q_f, R_q and R_f are all interpolated using serendipity basis functions. The quantities S_u, S_q (appearing in Q_q and Q_f) are incorporated as averaged values for each element, obtained by integrating equations (14) and (19), respectively over the element areas.[7] The usual Galerkin method is then applied to equations (6) and (7) whilst the algebraic relations (3) and (8) to (13) (having eliminated μ_t using equation (5)) are required to be satisfied pointwise at the grid nodes. In addition the normal gradients of equations (8) are required to be satisfied at the gradient nodes of types 3 and 4 elements. The discretization of the alternative f equation (15) is entirely analogous to that set out above, and the resultant set of discrete equations is set out in Appendix III.

The discretization described minimizes the complexity of the discrete equation system[16] whilst preserving as much as possible the described characteristics of the differential equations. For instance, if convection and secondary sources are neglected and type-2 elements are used, the discrete q-equation is linear in the nodal values $[q^2]_i$ (see Appendix III), and then demonstration of the existence and uniqueness of the solution for $[q^2]_i$ is a trivial matter. However, the numerical procedure will seek a solution for q_i (i.e. q_i and not

$[q^2]_i$ will be treated as the unknown) since this will occur in the convection term. This solution will obviously not be unique, for the equation is insensitive to the sign of q_i. However, ignoring convection, it is equally obvious that any negative q_i occurring in an iteration sequence can be corrected positive, so that the desired solution is obtained. The exception to this is when the unique solution for $[q^2]_i$ is negative at some node, in which case there is no real solution for q_i. This point will be returned to in section 7.2.

The properties of the non-linear discretized f-equations (either equation (7) or (15)) are illustrated in Appendix IV. For a single one-dimensional element, it is shown there how the above conditions on the diffusivity and source terms ensure the existence of a unique solution for f^2 when convection is neglected. However, as with the q-equation, the existence of a real solution for f on every node, for any grid, and for any set of boundary conditions, cannot be guaranteed. Again, this will be discussed in section 7.2.

5. WALL BOUNDARY TREATMENT

As pointed out in Reference 16, it is not convenient to calculate the momentum field right up to a solid wall, nor is the turbulence model valid in the near-wall region. The 'wall' part of the $\partial\Omega_1$ boundary is therefore understood to be displaced a small distance into the flow, where the fluid can be assumed to be fully turbulent. Conditions are then imposed on the boundary which match the interior flow to assumed behaviour in the wall region. The conditions adopted are the same as those in Reference 7 and therefore will only be explained briefly here. They are based on the logarithmic law of the wall, but with a modified scaling of the velocity and distance from the wall to ensure that sensible conditions are imposed at reattachment points. For the turbulence fields, it is assumed that there is a constant k $(=q^2)$ region near the wall where the length scale is proportional to wall distance.

If u, v are velocity components and x, y are local co-ordinates tangential and normal to the wall, respectively, the matching conditions are as follows:

$$u^+ = \frac{1}{\kappa} \ln y^+ + C \tag{21}$$

$$v^+ = \frac{\mathrm{d}}{\mathrm{d}x}\left(\frac{1}{\mathrm{Re}\, u_k}\right) y^+ u^+ \tag{22}$$

$$\frac{\partial q^2}{\partial y} = 0 \tag{23}$$

$$f = C_\mu^{1/2} u_k / \kappa y \tag{24}$$

where the scaling is defined by

$$u \text{ (or } v) = \frac{\tau_W}{u_k} u^+(v^+); \qquad y = \frac{1}{\mathrm{Re}\, u_k} y^+.$$

Here τ_W is the wall shear stress, u_k is given by $C_\mu^{1/4} q$ and the constants κ and C take their usual values 0·419 and 5·45, respectively.

These matching conditions are easily discretized using the normal velocity gradients ∂u_i, ∂v_i available at the wall nodes of type 3 and 4 elements. The discrete forms of equations (21) and (22) are[7]

$$u_i = \Delta h_i \, \partial u_i \, (\ln (C_\mu^{1/4} \, \mathrm{Re} \, \Delta h_i q_i) + \kappa C)$$
$$u_i v_i = \Delta h_i (u_i \, \partial v_i - v_i \, \partial u_i),$$

which are to be satisfied for every 'wall' node i, where Δh_i is the displacement of the node from the wall. Equation (24) is also applied pointwise, but (23) is imposed as a natural boundary condition by leaving q_i free at wall nodes. As pointed out in Reference 7, this is consistent with an equilibrium wall layer whilst placing minimum restriction on q where equation (23) is not strictly true (e.g. near a reattachment point).

6. SOLUTION OF THE DISCRETE SYSTEM

The discrete transport equations for q and f are numerically stable when considered separately (i.e. when S_u and l or q, respectively are held constant). Thus there is considerable advantage to be gained by treating them separately in the solution algorithm for the whole system. Furthermore, the coupling between certain of the equations in the system is not very strong. The turbulence variables only enter the dynamical equations through the diffusivity π_u and the wall boundary conditions. Similarly, the q variable only enters the f-equation through the diffusivity and wall conditions. Thus an algorithm which solves these equations separately, in sequence, should not only prove numerically stable at each stage, but should also converge rapidly overall.

For the procedure described below, two divisions are made between the variables, one between the dynamical variables ($\mathbf{u}$, p) and the turbulence, and another between the q and f turbulence variables. Within each group, the discrete equations are solved by Newton–Raphson (NR) iteration, with the linear system in each iteration being handled by a direct frontal method. These NR iterations are terminated when the error (defined as the maximum error in a variable divided by the maximum value of that variable) reaches some predetermined level E_{NR}. The full algorithm is then as follows:

Step 1

Make initial guesses for $\mathbf{u}$ (zero everywhere, say), μ_t (a constant, say) and l (proportional to wall distance or shear layer width, say). From these, derive guesses for q, f from equations (5) and (13).

Step 2

(i) Update π_u (equations (3) and (5))
(ii) Solve* the dynamical equations and update ($\mathbf{u}$, p)

Step 3 (Repeated until the q and f updates make changes of less than some value E_t)

(i) Solve* the f-equation and update f
(ii) Update l (equation (13))
(iii) Solve* the q-equation and update q

Step 4

Go back to step 2 unless changes in the variables are all less than some value E_0 (i.e. overall convergence is achieved).

In the above, solve* indicates an NR iteration sequence. Typical values of the accuracy criteria for best efficiency are $E_{NR} = 10^{-2}$, $E_t = 10^{-1}$ and $E_0 = 3 \times 10^{-4}$.

7. PERFORMANCE OF THE q–f CODE

7.1. *A sudden pipe-expansion*

The prediction of flow in an axisymmetric sudden pipe-expansion provides a good illustration of the performance of the q–f code. Figure 2 shows the geometry and basic

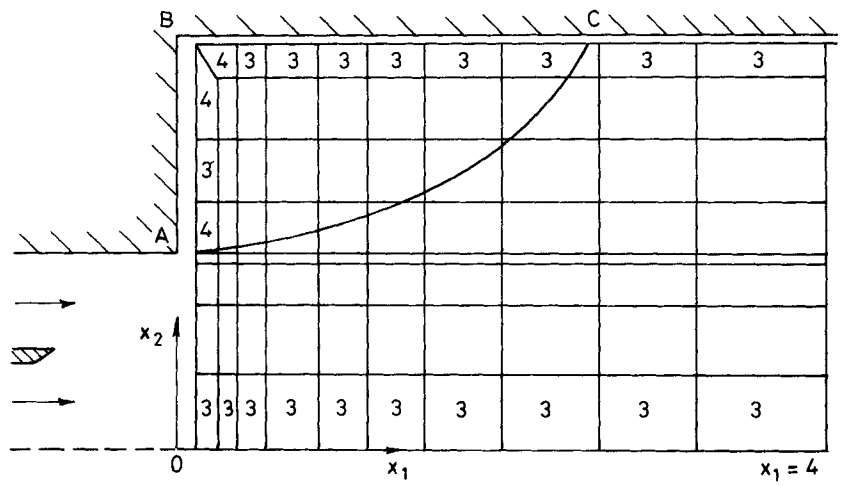

Figure 2. The jet-in-pool experiment (with FE grid)

features of the BNL Jet-in-Pool experiment[20,21] where a turbulent jet (coaxial with the pipe) emerges from a nozzle to mix with a slower moving annular stream. This results in complex inlet profiles for the subsequent pipe-expansion, which produces a shear layer spreading downstream from A, and a region of recirculation ABC with reattachment at C. The expansion ratio (downstream to upstream pipe diameter) is 0·476 and the Reynolds number based on diameter D and bulk velocity U downstream of the step is $6{\cdot}2\times10^4$.

Also illustrated in Figure 2 is the FE grid used for calculations. It consists of 79 quadrilateral elements displaced from the pipe wall by $\Delta h = 0{\cdot}02$ and displaced from the

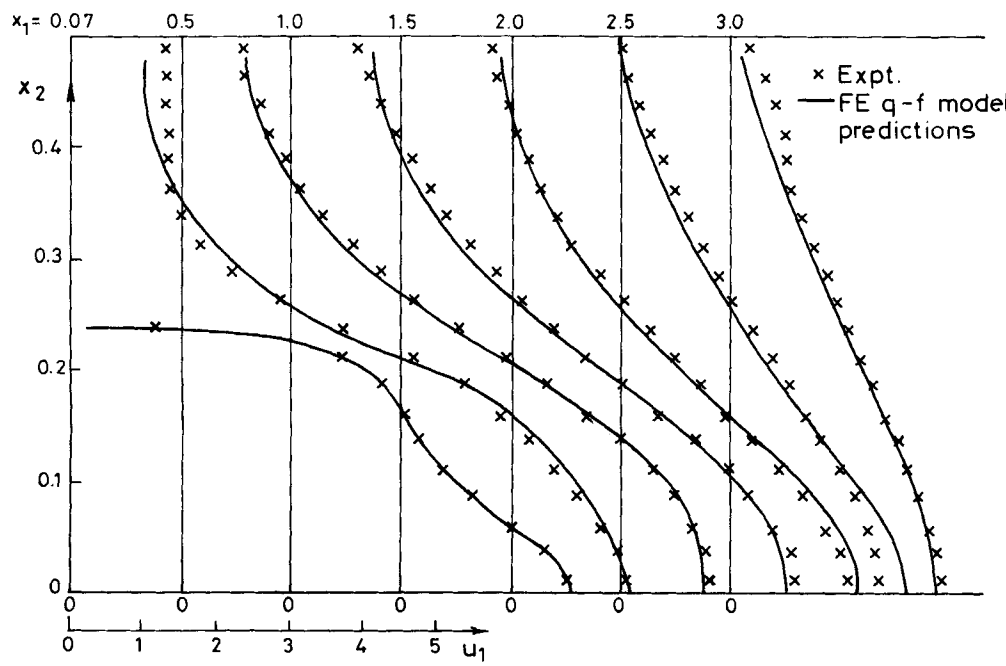

Figure 3. Axial velocity profiles compared with experiment

expansion face by $\Delta h = 0{\cdot}07$ (corresponding with the first measurement station in the experiments). The elements used were type 2 in the interior and types 3 and 4 at the edges as shown. Wall treatment was as described in section 5 except at the corner node near B, where the velocity components were set to zero. Experimental data for $\mathbf{u}$, q and f (where f and q were derived from measurements of normal and shear stresses and mean velocity gradients) were used as boundary conditions at inlet, and the outlet was left free so that the natural conditions zero surface traction and zero q^2 and f^2 normal gradients are satisfied there. On the symmetry axis, the normal gradients of u_1, f and q were set to zero explicitly.

As yet, there is no 'recommended' set of constants for the q–f model as there is for k–ε. Therefore C_{1f} (and hence σ_f through equation (20)) was adjusted to give a good fit of the centre-line u_1 prediction to experiment. A PALM penalty parameter of unity was found to give optimum continuity satisfaction. Then, with the values of the constants listed in section 3, the predictions for the u_1, q and l ($= C_\mu q/f$) fields (using the 'log' form of the f-equation (15)) are shown in Figures 3, 4 and 5. The agreement with experiment, especially for u_1 and l, is very good.

The initial guess used for the above calculation was $\mathbf{u} = 0$, $\mu_t/\mathrm{Re} = 1/70$ and $l = C_\mu^{1/4}\kappa y$ in the wall elements and constant in the interior. Convergence of the numerical scheme was achieved in 19 ($\mathbf{u}$, p) NR-iterations, 18 f NR-iterations and 18q NR-iterations, taking a total of 108 s on an IBM 3081 computer (which is approximately twice as fast as an IBM 370/168).

7.2. *Discussion*

The agreement of the q–f model results with experiment in the above example is very encouraging, though the model constants should obviously be fitted over a wider range of data before definite recommendations can be made. In particular, it was noticed that the

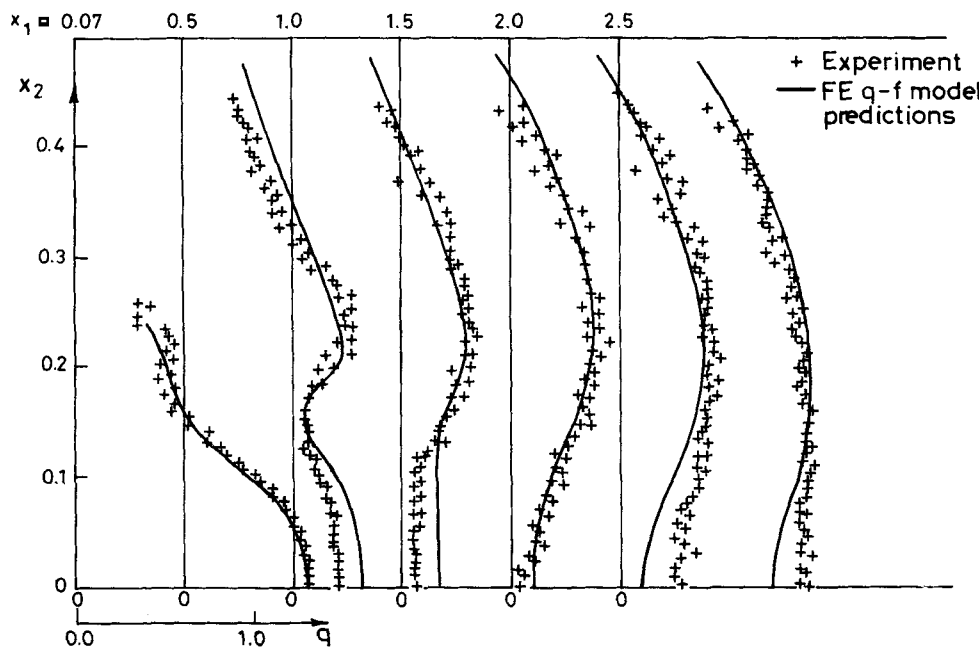

Figure 4. Profiles of q compared with experiment

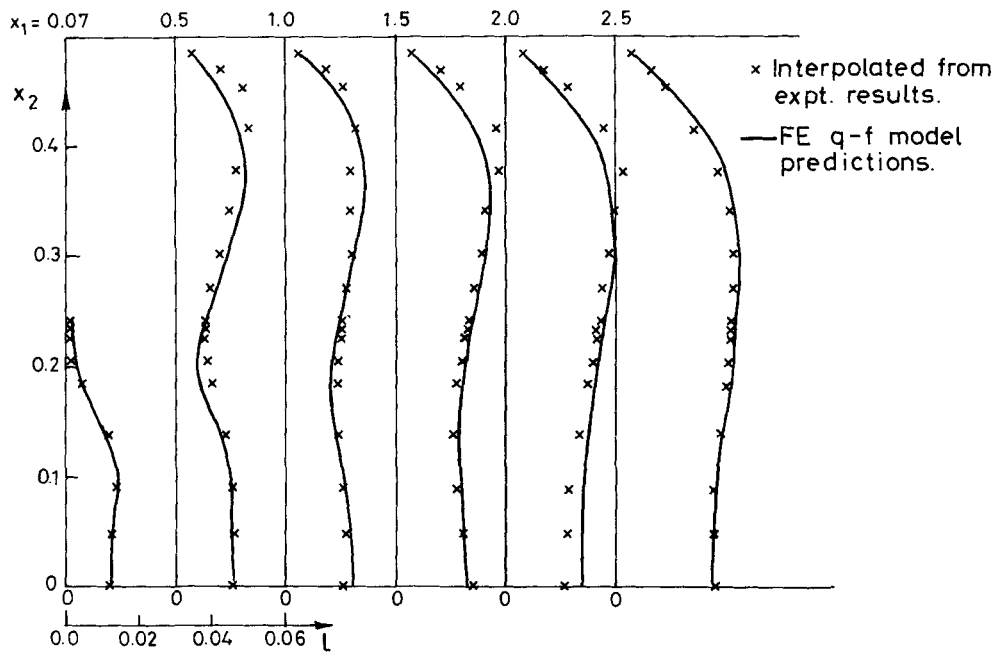

Figure 5. Length scale profiles compared with experiment

fitted value of C_{1f} was fairly sensitive to the inlet boundary conditions, in which there is inevitably some experimental uncertainty. Also, it is probable that for problems where wall effects exert a greater influence (e.g. flows with heat transfer) it will be necessary to improve the wall treatment near separation or reattachment points. However, it should be noted that the work in this paper does not rest entirely on the physical realism of the q–f model. Extra physical modelling can be accommodated in the secondary source term R_f. If such terms reduce the numerical stability of the f-equation, they can be added in the later stages of the solution algorithm, when the 'initial guess' is sufficiently good to ensure convergence.

The cost factor of the code (defined as the cost of a turbulent calculation compared with that of a laminar one on the same mesh) on the sudden pipe-expansion is approximately 5. The NR-procedure computer cost is proportional to (bandwidth)$^2 \times$(number of degrees of freedom) when the bandwidth is large. Thus a simultaneous solution of the system would have a cost factor of at least 8, even if it converged reliably. On a larger two-dimensional grid, the present algorithm has a cost factor of about 4, and in three dimensions this could be expected to be about 3, for the cost of q or f updates would then be negligible compared to $(\mathbf{u}, p)$. Considering that, as has been shown on the sudden-expansion example, good results can be obtained on fairly coarse meshes, this level of performance is extremely good.

As pointed out in section 4, it cannot be guaranteed that a real solution for q and f will exist on every node. No problems were experienced with the example solution given, but if the FE mesh cannot resolve a variation in q or f predicted by the turbulence model and large overshoots in the numerical approximation for q^2 or f^2 result, then that NR step may fail to converge. In practice, this can occur in the vicinity of 'difficult' boundary conditions, very near a re-entrant corner for instance. However, unlike the k–ε code described in Reference 7, the turbulence fields remain stable during the NR iterations in most of the flow, only showing large changes near the boundary causing the trouble. Thus, by monitoring the early

steps in the solution algorithm, inconsistent boundary conditions or areas of the mesh requiring refinement can be identified. This is entirely consistent with the usual methods of using Galerkin-FE codes, where (converged) spatial oscillations indicate the need for grid refinement.[22,23]

8. CONCLUSIONS

The q–f turbulence model and associated discretization method introduced in this paper have enabled a Galerkin-FE fluid-flow code to be constructed which is robust and efficient. This is in sharp contrast with similar codes based on the k–ε model. Furthermore, as has been demonstrated, the code can give good agreement with experiment on fairly coarse meshes.

It remains to test the applicability of the code in a wide range of geometries, and many changes and improvements are sure to emerge. However, such developments can be incorporated quite naturally into the computational framework presented here.

ACKNOWLEDGEMENT

This paper is published by permission of the Central Electricity Generating Board.

APPENDIX I

The relationship of the q–f model to the k–ε model

The q–f turbulence model used for the calculations in this paper has R_f set to zero. With other choices for R_f (and R_q defined by equation (18)), the equations can be made equivalent to other two-equation models. An example is the k–ε model.

The k–ε transport equations are

$$u_m \frac{\partial k}{\partial x_m} - \frac{1}{x_2^\alpha} \frac{\partial}{\partial x_m} \left(\frac{x_2^\alpha}{\sigma_k} C_\mu \frac{k^2}{\varepsilon} \frac{\partial k}{\partial x_m} \right) = C_\mu \frac{k^2}{\varepsilon} S_u - \varepsilon \tag{25}$$

$$u_m \frac{\partial \varepsilon}{\partial x_m} - \frac{1}{x_2^\alpha} \frac{\partial}{\partial x_m} \left(\frac{x_2^\alpha}{\sigma_\varepsilon} C_\mu \frac{k^2}{\varepsilon} \frac{\partial \varepsilon}{\partial x_m} \right) = C_\mu C_{1\varepsilon} k S_u - C_{2\varepsilon} \frac{\varepsilon^2}{k} \tag{26}$$

where the values of the constants C_μ, $C_{1\varepsilon}$, $C_{2\varepsilon}$, σ_k and σ_ε are 0·09, 1·44, 1·92, 1·0 and 1·3, respectively.[3] When ε is identified as $C_\mu q^3/l$ and $k = q^2$, it is easy to show that equation (25) is equivalent to the q-equation (6). By changing the variable in the ε-equation (26) from ε to f $(= \varepsilon/k)$ and q, one can show (after some manipulation) that equation (6) and (7) are equivalent to the k–ε model above if

$$R_f = \frac{C_\mu}{\sigma_\varepsilon} \frac{1}{f^2} \frac{\partial f^2}{\partial x_m} \frac{\partial q^2}{\partial x_m} - \frac{f}{x_2^\alpha q^2} \frac{\partial}{\partial x_m} \left(x_2^\alpha \mu_t \left(\frac{1}{\sigma_k} - \frac{1}{\sigma_\varepsilon} \right) \frac{\partial q^2}{\partial x_m} \right)$$

and the constants are modified to be

$$\sigma_f = \sigma_\varepsilon, \qquad C_{1f} = C_{1\varepsilon} - 1, \quad \text{and} \quad C_{2f} = C_{2\varepsilon} - 1.$$

APPENDIX II

Fitting of the q–f model constants to some idealized flows

In some simple flows, two-equation model transport equations can be solved analytically, enabling values of some of the constants to be fixed by reference to experiment (see Reference 8). Two examples are given below.

(i) *Decay of turbulence behind a grid.* It can be demonstrated experimentally that the turbulence energy in the flow downstream of a plane fine-wire grid varies as approximately the inverse of distance from the screen, x (i.e. $k \sim a^2 x^{-1}$, where a is some constant for a particular flow). Since the mean velocity u_g is uniform, the q and f transport equations (6) and (7) can be written

$$2u_g \frac{dq}{dx} = -qf \tag{27}$$

$$u_g \frac{df}{dx} = -C_{2f} f^2 \tag{28}$$

where the length scale has been eliminated and streamwise diffusion is ignored. Substituting $q \sim a x^{-1/2}$ into equation (27) gives $f \sim u_g x^{-1}$, and substituting this in turn into (28) yields the result that C_{2f} is approximately unity.

(ii) *Turbulent flow near a solid wall.* The fully turbulent flow near a solid wall has been well documented, and the main experimental characteristics are incorporated into the wall conditions given in section 5 of the paper. In addition, in equilibrium wall layers (e.g. away from separation and reattachment) convection is negligible and production of turbulence energy balances dissipation (e.g. see Reference 8), giving the result

$$\tau_W^{1/2} = u_k = C_\mu^{1/4} q, \text{ a constant.} \tag{29}$$

Equation (21) gives

$$\frac{du}{dy} = \frac{\tau_W}{\kappa u_k y} \tag{30}$$

and equation (24) is

$$f = C_\mu^{1/2} \frac{u_k}{\kappa y} \tag{31}$$

Then, substituting equations (29) to (31) into the f-transport equation (7) readily gives the relation

$$C_{1f} = C_{2f} - \frac{\kappa^2}{\sigma_f C_\mu^{1/2}}.$$

APPENDIX III

The discrete form of the q–f model equations

Using suffices i, j, etc. to denote nodal values (with the notation $[\ ]_i$ to denote the value of an expression at node i) and assuming the use of type 2 elements, the discretized q–f model equations are as follows.

The q-equation:

$$2u_{m,i}q_jB_{ijk,m}+\frac{1}{\sigma_q}l_i[q^2]_jA_{ijk,mm}=\left(\frac{2}{\sigma_q}[lS_q]_j+[lS_u]_j-C_\mu[q^2/l]_j\right)E_{jk} \tag{32}$$

the f-equation:

$$u_{m,i}f_jB_{ijk,m}+\frac{C_\mu}{2\sigma_f}[q^2/f^2]_i[f^2]_jA_{ijk,mm}=(C_\mu C_{1f}[S_u]_j-C_{2f}[f^2]_j)E_{jk} \tag{33}$$

with

$$l_j=C_\mu[q/f]_j \tag{34}$$

The alternative form of the f-equation (15) gives the following discrete form:

$$u_{m,i}f_jB_{ijk,m}+\frac{C_\mu}{2\sigma_f}[q^2]_i[\ln f^2]_jA_{ijk,mm}=(C_\mu C_{1f}[S_u]_j-C_{2f}[f^2]_j)E_{jk} \tag{35}$$

The momentum diffusivity is given by

$$[\pi_u]_j=\left[\frac{1}{\mathrm{Re}}+C_\mu\frac{q^2}{f}\right]_j \tag{36}$$

The matrix quantities A, B and E are defined by

$$A_{ijk,mn}=\int_\Omega W_i\frac{\partial W_j}{\partial x_m}\frac{\partial W_k}{\partial x_n}\,\mathbf{dx}$$

$$B_{ijk,m}=\int_\Omega W_i\frac{\partial W_j}{\partial x_m}W_k\,\mathbf{dx}$$

$$E_{ij}=\int_\Omega W_iW_j\,\mathbf{dx}$$

where $W_i(\mathbf{x})$ are serendipity basis functions.[17] The nodal values of S_u, S_q appearing in equations (32) and (33) are defined by:

$$[S_u]_i=\frac{\sum_e(S_u)_e}{\sum_e\int_{\Omega_e}\mathbf{dx}},\qquad [S_q]_i=\frac{\sum_e(S_q)_e}{\sum_e\int_{\Omega_e}\mathbf{dx}}$$

where the summations range over all the elements e sharing node i, and Ω_e denotes the region covered by element e. The area-weighted averages $\overline{(S_u)}_e$ and $\overline{(S_q)}_e$ are calculated from

$$\overline{(S_u)}_e=u_{n,i}u_{n,j}\int_{\Omega_e}\frac{\partial W_i}{\partial x_m}\frac{\partial W_j}{\partial x_m}\,\mathbf{dx}+u_{n,i}u_{m,j}\int_{\Omega_e}\frac{\partial W_i}{\partial x_m}\frac{\partial W_j}{\partial x_n}\,\mathbf{dx}+2\alpha u_{2,i}u_{2,j}\int_{\Omega_e}\frac{W_iW_j}{x_2^2}\,\mathbf{dx} \tag{37}$$

and

$$\overline{(S_q)}_e=q_iq_j\int_{\Omega_e}\frac{\partial W_i}{\partial x_m}\frac{\partial W_j}{\partial x_m}\,\mathbf{dx}. \tag{38}$$

APPENDIX IV

Single element discretizations of the f-equation

Consider a one-dimensional f-equation (in interval $0\leq x\leq 1$, say) with convection neglected, $R_f=0$ and, for simplicity, with the diffusivity given by $\pi=\pi'/f^2$, where π' is constant.

Equation (7) then becomes:

$$-\frac{\mathrm{d}}{\mathrm{d}x}\left(\pi\frac{\mathrm{d}F}{\mathrm{d}x}\right)=C_\mu C_{1f}S_u-C_{2f}F \tag{39}$$

where

$$F=f^2 \tag{40}$$

If π and F are interpolated using quadratic one-dimensional versions $W_i(x)$ of type 2 element basis functions (i being the node label), the FE discretization procedure yields

$$\pi'\frac{F_k}{F_i}\int_0^1 W_i\frac{\mathrm{d}W_k}{\mathrm{d}x}\frac{\mathrm{d}W_j}{\mathrm{d}x}\,\mathrm{d}x=C_\mu C_{1f}\int_0^1 S_u W_j\,\mathrm{d}x-C_{2f}F_k\int_0^1 W_k W_j\,\mathrm{d}x \tag{41}$$

where F_j is the value of F(or f^2) at node j. For a single element ($1\leq j\leq 3$), with the boundary nodes fixed at $F_1=\alpha>0$ and $F_3=\beta>0$, respectively, equation (41) reduces to a simple quadratic equation for the single unknown F_2:

$$aF_2^2+bF_2+c=0 \tag{42}$$

where

$$a=12(\alpha+\beta)/\alpha\beta+16C_{2f}/\pi'$$
$$b=6+15C_0/\pi'+(\alpha^2+\beta^2)/\alpha\beta-2C_{2f}(\alpha+\beta)/\pi'$$
$$c=-8(\alpha+\beta)$$

and

$$C_0=C_\mu C_{1f}\int_0^1 S_u W_2\,\mathrm{d}x>0.$$

The solutions of equation (42) are obviously

$$F_2=-\frac{b}{2a}\left[1\pm\sqrt{\left(1-4\frac{ac}{b^2}\right)}\right].$$

Consider now three situations:

(i) *Diffusivity greater than zero, sources monotonic decreasing in F*

When $\pi'>0$ and $C_{2f}>0$, the quantity $ac<0$ and thus there are two solutions for F_2, one negative and one positive. But since F_2 is defined by f_2^2 where f_2 is assumed real, only the positive F_2 is admissible. Thus, there is a unique solution for F_2.

(ii) *Diffusivity less than zero, sources monotonic decreasing in F*

When $\pi'<0$ and $C_{2f}>0$, there is the possibility (if $|\pi'|<4C_{2f}\alpha\beta/3(\alpha+\beta)$) that $ac>0$, and then both solutions of (42) will be of the same sign. The sign could be positive or negative according to the size of C_0. The former would imply two solutions for F_2 (and hence f_2^2), and the latter would imply that there are no real solutions for f_2.

(iii) *Diffusivity greater than zero, sources monotonic increasing in F*

When $\pi'>0$ and $C_{2f}<0$, there is again the possibility that $ac>0$. Both solutions of F_2 are then positive and two solutions for f_2^2 exist.

Summarizing the above results, it is clear that for a single one-dimensional element, sufficient conditions for the existence of a unique discrete solution for f^2 are that diffusivity is positive and that the source term is monotonic decreasing in F. If either of these conditions is relaxed, there is a possibility that the solution is not unique or that no real solution for f exists.

The alternative form of the f equation (15) reduces to the following discrete equations under the assumptions described above:

$$\pi' \ln F_k \int_0^1 \frac{dW_k}{dx}\frac{dW_j}{dx}\,dx = C_\mu C_{1f}\int_0^1 S_u W_j\,dx - C_{2f}F_k\int_0^1 W_k W_j\,dx \tag{43}$$

On a single element, this becomes

$$\ln F_2 = -AF_2 + B \tag{44}$$

where

$$A = \tfrac{2}{5}C_{2f}\alpha/\pi'$$

and

$$B = \tfrac{1}{2}(\ln\alpha + \ln\beta - C_{2f}(\alpha+\beta)/10\pi' + 3C_0/4\pi').$$

It is then easy to show, by simple graphical arguments, that the above results are also valid for this discretization.

REFERENCES

1. C. Taylor, K. Morgan and C. A. Brebbia (eds.), *Numerical Methods in Laminar and Turbulent Flow*, Proc. 1st International Conf., Pentech Press, London, 1978.
2. D. H. Norrie (ed.), *Finite Elements in Flow Problems*, Proc. 3rd International Conference, Banff, Canada, 1980.
3. W. Rodi, 'Turbulence models and their application in hydraulics', *IAHR State-of-the-Art Paper*, Delft, Netherlands (1980).
4. A. D. Gosman, W. M. Pun, A. K. Runchal, D. B. Spalding and M. Wolfshtein, *Heat and Mass Transfer in Recirculating Flows*, Academic Press, London, 1969.
5. B. E. Larock and D. R. Schamber, 'Approaches to the finite element solution of two-dimensional turbulent flows', in *Computational Techniques in Transient and Turbulent Flow* (eds. C. Taylor and K. Morgan), Pineridge Press, 1981.
6. G. D. Tong, 'Computation of turbulent recirculating flow', *Ph.D. Thesis*, Dept. Civil Engineering, University College of Swansea, U.K., 1982.
7. R. M. Smith, 'On the finite-element calculation of turbulent flow using the k–ϵ model', *Int. j. numer. methods fluids*, **4**, 303–319 (1984).
8. B. E. Launder and D. B. Spalding, *Lectures in Mathematical Models of Turbulence*, Academic Press, London, 1972.
9. A. N. Kolmogorov, 'Equations of turbulent motion of an incompressible turbulent fluid', *Izv. Akad, Nauk SSSR Ser. Phys. VI*, No. 1–2, 56–58 (1942).
10. D. B. Spalding, 'The $k \sim W$ model of turbulence', *Imperial College Mechanical Engineering Dept. Report TM/TN/A/16*, London (1972).
11. P. G. Saffman, 'A model for inhomogeneous turbulent flow', *Proc. Roy. Soc.* Ser. **A317**, 417–433 (1970).
12. D. C. Wilcox and R. M. Traci, 'A complete model of turbulence', *AIAA Paper 76–351*, AIAA 9th Fluid and Plasma Dynamics Conference, San Diego, California (1976).
13. D. Bryant and J. A. C. Humphrey, 'Conservation equations for laminar and turbulent flows in general three-dimensional co-ordinates', *Imperial College Mechanical Engineering Dept. Report CHT/76/2*, (1976).
14. B. E. Launder and D. B. Spalding, 'The numerical computation of turbulent flows', *Computer Meth. in Appl. Mech. and Engng.*, **3**, 269–289 (1974).
15. A. G. Hutton, 'A survey of the theory and application of the finite element method in the analysis of viscous incompressible Newtonian flow', *CEGB Report RD/B/N3049* (1974).
16. A. G. Hutton and R. M. Smith, 'On the finite element simulation of incompressible turbulent flow in general two-dimensional geometries', *CEGB Report RD/B/5010N81*, also in *Numerical Methods in Laminar and Turbulent Flow* (eds. C. Taylor and B. A. Schrefler), Pineridge Press, 1981.
17. O. C. Zienkiewicz, *The Finite Element Method*, 3rd edn, McGraw-Hill, London, 1977.
18. A. G. Hutton, 'Finite element boundary techniques for improved performance in computing Navier–Stokes and related heat transfer problems', in *Finite Elements in Fluids Vol.* 4 (ed. R. H. Gallagher, D. H. Norrie, J. T. Oden and O. C. Zienkiewicz), Wiley, Chichester, 1982, pp. 433–452.
19. G. H. Meyer, 'The numerical solution of quasilinear elliptic equations', in *Numerical Solution of Systems of Nonlinear Algebraic Equations* (eds. G. D. Byrne and C. A. Hall), Academic Press, New York, 1973.
20. A. R. Freeman and R. T. Szczepura, 'Mean and turbulent velocity measurements in an abrupt axisymmetric pipe expansion with a complex inlet geometry', in *Proceedings of the International Symposium on the Applications of Laser Doppler Anemometry to Fluid Mechanics*, Lisbon, Portugal, July 1982.

21. R. T. Szczepura, 'The Reynolds number dependence of the velocity field in the BNL jet-in-pool water experiments', *CEGB Report RD/B/4999N81* (1981).
22. P. Gresho and R. L. Lee, 'Don't suppress the wiggles—they're telling you something', in *Finite Element Methods for Convection Dominated Flows* (ed. T. J. R. Hughes), American Society for Mech. Engs. AMD-Vol. 34, 1979, p. 37.
23. R. M. Smith and A. G. Hutton, 'The numerical treatment of advection—a performance comparison of current methods', *Numerical Heat Transfer* **5,** 439–461, also *CEGB Report TPRD/B/0001/N82* (1982).